Structure of Adsorbed Polymers on a Colloid Particle

Shuang Yang and Dadong Yan*

Beijing National Laboratory for Molecular Sciences (BNLMS), Joint Laboratory of Polymer Science and Materials, Institute of Chemistry, Chinese Academy of Sciences, Beijing 100080, China

An-Chang Shi[†]

Department of Physics and Astronomy, McMaster University, Hamilton, Ontario L8S 4M1, Canada

Received January 3, 2006; Revised Manuscript Received April 14, 2006

ABSTRACT: The adsorption of homopolymers on spherical particles with a strong attractive potential has been studied using the self-consistent field theory. The particles are immersed in concentrated polymer solutions and the structure of the adsorbed polymer layer has been examined as a function of the particle size, focusing on the average loop and tail length at different bulk concentrations and solvent qualities. The scaling relationship between the average tail/loop length and the degree of polymerization has been investigated. It is found that the average loop length is insensitive to the particle size or surface curvature. However, the average tail length depends strongly on the particle size. In particular, tails become longer for smaller particles or larger surface curvatures. It is argued that this size effect may provide a mechanism for the excess entanglements induced by adding nanoparticles to polymer solutions.

1. Introduction

Mixtures of colloid suspensions and polymers are widely used in many industrial applications. Examples include adhesion and lubrication.[1] In many cases polymers can interact strongly with the colloidal particles. If one monomer is adsorbed by the particle surface, there is an enhanced probability that many others are also adsorbed on the surface due to the chain connectivity. Therefore, polymers can be strongly attracted by the particles. The adsorbed polymer conformation can be described in terms of loops and tails.[2] There are two possible applications of the adsorption between polymers and colloids. One application is to control the stability of colloidal suspensions by adding adsorbed polymers, such as in paints or in wastewater treatment. In fact the interaction between two dispersions carrying adsorption layers is rather subtle. It depends on the precise conformation of the polymer chains on the surface, and strongly on the reversibility of the adsorption. In the restricted equilibrium regime and good solvent solutions, because of the excluded volume interactions the adsorbed polymer layers on two adjacent particles repel each other and stabilize the colloidal dispersions. If a polymer chain is long enough, it can link different particles and flocculate them through bridges. The other application is to improve the rheological and mechanical properties of the system by adding small amount of nanoparticles to polymer solutions and melts. Since loops and tails of adsorbed polymers are dangling from the surface into solutions, one chain connects several particles when bridges occur between long polymer chains and colloids. In this case, the polymer composite becomes a gel where colloids act as cross-links.[3] However, if the chains are not long enough, even if no bridge occurs, the properties of polymer composite can be affected by entanglements between tails and loops belonging to different particles. This entanglement mechanism is different from those appearing in bulk, which are caused by long free polymer chains. The solution can also become a large polymer gel as if it is cross-linked by those nanoparticles. The rheology of the polymer solution and melt may be affected strongly by the addition of nanoparticles. For example, the viscosity of the polymer solution can be increased greatly. The key factor is the conformation of the adsorbed polymers. One interesting question is why adding a small amount of nanoparticles has a large effect. It is obvious that the size of the particles matters in these applications. Therefore, it is of great interest to investigate the effect of particle size or surface curvature on polymer adsorption. A few studies on how curvature affects the conformation of polymer near curving surfaces have appeared in the literature. Wijmans and Zhulina investigated the curvature effect on the density profile of polymer brushes at the curved surface.[4] Aubouy and Raphael presented a scaling description for the behavior of loops and tails of polymers adsorbed on a spherical surface.[5] Also, Ji and Hone[6] and Skau and Blokhuis[7] focused on the structural properties of adsorbed polymers and took into account the weak curvature effects as a perturbation.

The equilibrium structure of homopolymers reversibly adsorbed on flat surfaces has been investigated theoretically for many years. Early theoretical treatment of a polymer solution in the vicinity of a solid surface was a mean field theory based on the ground state dominant approximation (GSA).[8−10] In this approximation, the chain end effect is ignored and the polymer chain is treated as infinitely long. Furthermore, de Gennes proposed a scaling theory beyond the mean field theory.[8,11,12] This theory grasps the spirit of self-similar structure of adsorbed polymers and predicts the main qualitative features of adsorbed layer successfully. Eisenriegler et al. derived various scaling results and the universal amplitude ratios about polymer adsorption with excluded volume interaction using the analogy with the zero-component field theory.[13−15] Scheutjens and Fleer et al. developed a lattice model, which can be used to describe many aspects of polymer adsorption.[1,16,17] The statistical distribution of tails and loops can be enumerated easily, highlighting the influence of tails and loops on experimentally observable quantities. The tails mostly builds up the external part of adsorbed layer, whereas the loops are the main part close to the wall. Recently, Semenov et al. proposed a two-parameter theory, which is a modified version of the mean field theory

---

* Corresponding author. E-mail: yandd@iccas.ac.cn.
[†] E-mail: shi@mcmaster.ca.

10.1021/ma060014a CCC: $33.50

and presents the importance of the chain ends.[18,19] In the most recent publications, Daoulas et al. proposed a self-consistent field theory (SCFT) treatment about compressible semiflexible polymer adsorption.[20] They presented the chain connectivity through the wormlike chain model. Later, Mavrantzas et al. developed the continuum formulation of the Scheutjens−Fleer (SF) lattice statistical theory for homopolymer adsorption from solution. It is a hybrid description combing the continuous space formula and the original SF lattice model.[21]

In certain situations tails become important and lead to qualitatively different behavior.[19,22] For example, the effect of chain ends may change the interaction between two plates from attractive to repulsive when the separation is large enough. In fact, we will find that tails are more important than loops in the out space of adsorbed layer. Furthermore, tails determine the hydrodynamic thickness of adsorbed polymer layer[23] and the excess entanglements in out space of adsorbed layer. Tails may also seriously affect the interplay between two colloidal particles with adsorbed polymers. In this case the curvature of nanoparticles becomes more important. Therefore, we should focus on the influence of surface curvature on the tails.

In this paper, SCFT is employed to calculate the structure of polymer layer adsorbed on a spherical particle in polymer solutions. The method used in this paper is based on the work of Noolandi et al.[24,25] In their method the self-consistent equations are constructed in continuous spaces, and then discretized and solved numerically. This method is convenient since it can be cast easily in different coordinate systems. The essence of this method is the same as the lattice model developed by Fleer et al.[2]

This paper is organized as follows. In the next two sections, we outline the SCFT for adsorption and the method to solve the equations numerically. The polymer density profile, average loop and tail length are computed for different particle sizes and different bulk concentrations. We also study the scaling relationship between the average length of tail/loop and the degree of polymerization for different curvatures. In the section of discussion we argue the possible applications of varying the properties of polymer solution by adding small colloid particles to form excess entanglement. Conclusions are presented in the last section.

2. Theoretical Framework

We consider a system in which a nanoparticle with radius R is immersed in a polymer solution. The particle surface is impenetrable and the adsorption is reversible. N denotes the degree of polymerization. The indices p and s are used to label the polymer and solvent molecules, respectively. We take the Kuhn length b associated with polymer segment as the unit of length. The interactions between polymer segments and solvent molecules are described by a Flory−Huggins parameter χ. The canonical ensemble is used. With the self-consistent field theory the partition function of the system is given by[24]

$$Z = \int \prod_i (\mathscr{D}\phi_i \mathscr{D}\omega_i) \prod_{\mathbf{r}} \delta[\phi_{\mathrm{p}}(\mathbf{r}) + \phi_{\mathrm{s}}(\mathbf{r}) - 1] \mathrm{e}^{-F(\{\phi\},\{\omega\})} \qquad (1)$$

$$\frac{F(\{\phi\},\{\omega\})}{\rho_0 k_{\mathrm{B}} T} = \int \mathrm{d}\mathbf{r}\, [\chi \phi_{\mathrm{p}}(\mathbf{r})\phi_{\mathrm{s}}(\mathbf{r}) - \omega_{\mathrm{p}}(\mathbf{r})\phi_{\mathrm{p}}(\mathbf{r}) - \omega_{\mathrm{s}}(\mathbf{r})\phi_{\mathrm{s}}(\mathbf{r}) + U(\mathbf{r})\phi_{\mathrm{p}}(\mathbf{r})] - \frac{n_{\mathrm{p}}}{\rho_0} \ln \frac{\rho_0 Q_{\mathrm{p}}(\{\omega_{\mathrm{p}}\})}{N n_{\mathrm{p}}} - \frac{n_{\mathrm{s}}}{\rho_0} \ln \frac{\rho_0 Q_{\mathrm{s}}(\{\omega_{\mathrm{s}}\})}{N n_{\mathrm{s}}} \qquad (2)$$

where n_{p} and n_{s} are the number of polymers and the number of solvents, respectively; ρ_0 is a reference monomer density; $\phi_\alpha(\mathbf{r})$ is the inhomogeneous volume fraction of polymer or solvent with the corresponding mean field $\omega_\alpha(\mathbf{r})$, where $\alpha = \mathrm{p}$ and s, respectively; Q_α is the single chain partition function. We ignore the interaction between solvents and particle for simplicity. It is assumed that between the polymer monomer and the surface there exists a short-range adsorption interaction which extend over distance on the order of chain unit size. The adsorbing potential $U(\mathbf{r})$ is assumed to be a rectangular-form potential for simplicity. In spherical coordinates, it is assumed to have the form as follows

$$U(r) = \begin{cases} 0 & r > R + d \\ -U_0 & R \le r \le R + d \end{cases}$$

where d is on the order of b.

Using the saddle-point approximation, we can obtain a set of self-consistent equations including densities and fields. The key quantity of the theory is the propagator $q(\mathbf{r}, t)$, which describes the probability distribution of the tth monomer at position $\mathbf{r}$. $q(\mathbf{r}, t)$ can be obtained by solving the modified diffusion equation

$$\frac{\partial}{\partial t} q(\mathbf{r}, t) = \frac{b^2}{6} \nabla^2 q(\mathbf{r}, t) - \omega_{\mathrm{p}}(\mathbf{r}) q(\mathbf{r}, t) \qquad (3)$$

where $\omega_{\mathrm{p}}(\mathbf{r})$ is the mean field acting on the polymers. The initial condition of the propagators is

$$q(\mathbf{r}, 0) = 1 \qquad (4)$$

and the boundary conditions are

$$q(\mathbf{r}, t)|_{\mathbf{r}=\mathrm{R}} = 0$$
$$q(\mathbf{r}, t)|_{\mathbf{r}\to\infty} = 1 \qquad (5)$$

Here, we use the fact that adding a constant to the mean field does not change the polymer density profile. So we can normalize the propagators by propagators of bulk $q^{\mathrm{bulk}}(\infty, t)$, or, $q(\mathbf{r}, t) = q^{\mathrm{real}}(\mathbf{r}, t)/q^{\mathrm{bulk}}(\infty, t)$. Thus, at infinite distance the mean field can always be taken as zero.

The polymer and solvent concentrations are given by

$$\phi_{\mathrm{p}}(\mathbf{r}) = \frac{n_{\mathrm{p}}}{\rho_0 Q_{\mathrm{p}}} \int_0^N \mathrm{d}t\, q(\mathbf{r}, t) q(\mathbf{r}, n - t) \qquad (6)$$

$$\phi_{\mathrm{s}}(\mathbf{r}) = \frac{n_{\mathrm{s}}}{\rho_0 Q_{\mathrm{s}}} \mathrm{e}^{-\omega(\mathbf{r})} \qquad (7)$$

The partition functions of a single polymer chain and a solvent are given by

$$Q_{\mathrm{p}} = \int \mathrm{d}\mathbf{r}\, q_{\mathrm{p}}(\mathbf{r}, N) \qquad (8)$$

$$Q_{\mathrm{s}} = \int \mathrm{d}\mathbf{r}\, \mathrm{e}^{-\omega_{\mathrm{s}}(\mathbf{r})} \qquad (9)$$

The mean fields $\omega_{\mathrm{p}}(\mathbf{r}, t)$ are given in terms of the volume fractions by the following equations

$$\omega_{\mathrm{p}}(\mathbf{r}) = \chi[\phi_{\mathrm{s}}(\mathbf{r}) - \phi_{\mathrm{s}}{}^0] + U(\mathbf{r}) + \eta(\mathbf{r}) \qquad (10)$$

$$\omega_{\mathrm{s}}(\mathbf{r}) = \chi[\phi_{\mathrm{p}}(\mathbf{r}) - \phi_{\mathrm{p}}{}^0] + \eta(\mathbf{r}) \qquad (11)$$

where $\phi_{\mathrm{p}}{}^0$ and $\phi_{\mathrm{s}}{}^0$ are the bulk concentration of polymer and solvent, respectively. The function $\eta(r)$ is to be adjusted to ensure the incompressibility condition

$$\phi_p(\mathbf{r}) + \phi_s(\mathbf{r}) = 1 \qquad (12)$$

The above SCFT equations are highly nonlinear, and we must discretize the space and solve these equations by numerical iteration method. As this system is spherical symmetry, all quantities are functions of r only. Starting with an initial trial fields, $\omega_p{}^0(r_i)$ and $\omega_s{}^0(r_i)$, we can obtain $q_p(r_i, t_j)$ from eqs 3−5. The process of solving the modified diffusion equation in sphere coordinate is presented in the Appendix. Then the density profiles $\phi_p(r_i)$ and $\phi_s(r_i)$ are calculated from eqs 6 and 7. From the densities, a new set of mean fields can be obtained from eqs 10−12. The process is repeated until the self-consistent solutions for $\phi_p(r_i)$ and $\phi_s(r_i)$ are reached.

Once the density profiles and the mean field values are obtained, we can calculate the Green function of the polymer chains, $G(\mathbf{r},\mathbf{r}';0, t)$, which describes the statistical weight of a single chain of length t with one end at $\mathbf{r}$ and the other end at $\mathbf{r}'$. It can be determined by solving the modified diffusion equation

$$\frac{\partial}{\partial t}G(\mathbf{r},\mathbf{r}';0, t) = \frac{b^2}{6}\nabla^2 G(\mathbf{r},\mathbf{r}';0, t) - \omega_p(\mathbf{r})G(\mathbf{r},\mathbf{r}';0, t) \qquad (13)$$

with initial condition

$$\lim_{t\to 0} G(\mathbf{r},\mathbf{r}';0, t) = \delta(\mathbf{r} - \mathbf{r}') \qquad (14)$$

which is the same as $q(\mathbf{r}, t)$ except for the initial condition. They are related by

$$q(\mathbf{r}, t) = \int \mathrm{d}\mathbf{r}'\, G(\mathbf{r},\mathbf{r}';0, t) \qquad (15)$$

To calculate the structure of adsorbed polymer with imposed boundary condition $\phi_p(\mathbf{r})|_{\mathbf{r}=R} = 0$, we need to define the adsorbed layer profile as follows. At the surface of a particle the density profiles of the polymers are zero. Between the surface of the particle and the infinite distance the density profile has a maximum and two inflections. The distance from origin to the second inflection, which is between the infinite distance and the sphere where the density profile has the maximum, is denoted by r_w. The region between the surface of the particle and the sphere corresponding to the location of r_w is called the boundary layer. The region outside the boundary layer is defined as the adsorbed layer, where the polymer density is higher than that in bulk solution. Our calculation shows that the difference between r_w and $R + d$ is rather small. Typically it is smaller than the Kuhn length b. We can then divide the adsorbed layer into two parts. One is the adsorbed part, while the other is the free part. A polymer will be an adsorbed polymer if any part of it falls into the boundary layer. The free polymers are those with none of their segments in the boundary layer. The total propagator $q(\mathbf{r}, t)$ can be divided into the adsorbed and free ones, $q(\mathbf{r}, t) = q^a(\mathbf{r}, t) + q^f(\mathbf{r}, t)$. The propagator of the adsorbed chain $q^a(\mathbf{r}, t)$ and the propagator of the free chain $q^f(\mathbf{r}, t)$ satisfy the same modified diffusion equations as $q(\mathbf{r}, t)$, but with different boundary conditions. The propagator of free chain vanishes at the adsorb layer wall, $q(\mathbf{r}, t)|_{\mathrm{r}=\mathrm{r}_w} = 0$. The propagator of adsorbed polymer $q^a(\mathbf{r}, t)$ can be obtained from $q^f(\mathbf{r}, t)$. Using the propagators of the adsorbed chain and free chains we can split the total volume fraction into three parts, i.e., tail, loop and free parts. The volume fraction of segments coming from loops, tails and free chains are given by

$$\phi^l(\mathbf{r}) = \frac{\phi_p{}^0}{N}\int \mathrm{d}t\, q^a(\mathbf{r}, t)q^a(\mathbf{r}, N - t) \qquad (16)$$

$$\phi^t(\mathbf{r}) = \frac{\phi_p{}^0}{N}\int \mathrm{d}t\, q^a(\mathbf{r}, t)q^f(\mathbf{r}, N - t) \qquad (17)$$

and

$$\phi^f(\mathbf{r}) = \frac{\phi_p{}^0}{N}\int \mathrm{d}t\, q^f(\mathbf{r}, t)q^f(\mathbf{r}, N - t) \qquad (18)$$

Similarly, we can divide the Green functions into two parts, or, $G(\mathbf{r},\mathbf{r}';0, N) = G^a(\mathbf{r},\mathbf{r}';0, N) + G^f(\mathbf{r},\mathbf{r}';0, N)$. To calculate the average loop and tail length we only need to calculate $G^f(R + r_w, R + r_w; 0, N)$, which gives the weight of a chain with two ends at r_w and the other monomers dangling out of the adsorbed layer. It has the same meaning as the tail end segment distribution function $G^t(z, s)$ introduced by Fleer et al.[2]

To find the average tail length l_{tail} and the average loop length l_{loop} we discretize the space and then calculate these quantities using a method developed for the lattice model.[2] Each unit length is equal to one lattice size. The out spherical surface of the boundary layer is denoted as the kth layer, and then the (k + 1)th layer is the boundary of free chains. Thus, we have

$$l_{\mathrm{tail}} = \frac{\sum_{t=0}^{N\text{-}1} t q^f(k + 1, t)q^a(k, N - t - 1)}{\sum_{t=0}^{N\text{-}1} q^f(k + 1, t)q^a(k, N - t - 1)} \qquad (19)$$

$$l_{\mathrm{loop}} = \frac{\sum_{s=0}^{N\text{-}n\text{-}2}\sum_{t=0}^{N\text{-}2} t q^a(k + 1, t)G^f(k + 1, K + 1; 0, t)q^a(k, N - t - 1)}{\sum_{s=0}^{N\text{-}n\text{-}2}\sum_{t=0}^{N\text{-}2} q^a(k + 1, t)G^f(k + 1, K = 1; 0, t)q^a(k, N - t - 1)} \qquad (20)$$

In the above definition, the average tail length is the average number of segments belong to tail. The definition for loop is the same as tail.

The tail fraction ν_{tail} can be integrated by

$$\nu_{\mathrm{tail}} = \frac{\int \mathrm{d}\mathbf{r}\, \phi^t\{\mathbf{r}\}}{\int \mathrm{d}\mathbf{r}\, \phi_p\{\mathbf{r}\}} \qquad (21)$$

and the loop fraction can be obtained from

$$\nu_{\mathrm{loop}} = 1 - \nu_{\mathrm{tail}} \qquad (22)$$

3. Results

Before presenting our results, we would like to discuss the applicability of the SCF theory of polymer solutions. As a mean-field theory, our model is appropriate for systems close to the theta point. The limitation of the mean-field theory in polymer solutions can be stated in terms of polymer concentration and the related excluded-volume parameter (or the Flory interaction parameter of χ). A common estimate of the validity of mean-field theory is due to Edwards,[26] who gave a criterion in terms of the Ginzburg parameter, which leads to the conclusion that the mean-field theory is valid if $c \geq c^{**} \approx \upsilon/b$.[6] The

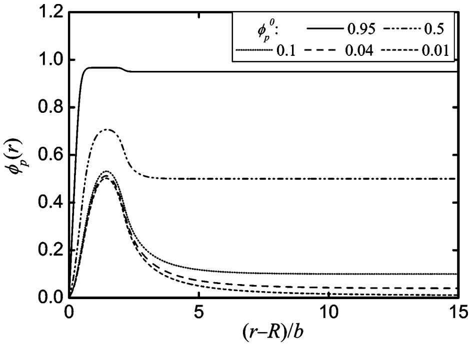

Figure 1. Polymer density profile $\phi_p(\mathbf{r})$ near the surface of a particle at different polymer bulk concentrations of $\phi_p{}^0 = 0.01$, 0.04, 0.1, 0.5, and 0.95, respectively. The parameters are $N = 1000$, $\chi = 0.4$, and $R/b = 10$.

effective excluded volume v is related to the Flory−Huggins parameter χ by $v = (1 - 2\chi)b^3$ at the mean field level for small concentrations. Using the Edwards criterion, we conclude that c^{**} is rather small for χ near to 0.5. Therefore, the mean field theory is applicable for χ near to 0.5, as well as for the concentrated solutions with $\phi_p{}^0$ near to 1. On the other hand, using the scaling arguments Schaefer concluded that the mean field theories describe the properties of polymers in solution correctly over a wider range of concentration and solvency.[27,28] He gave a concentration limit of $\tilde{\phi}$, which is given by $\tilde{\phi} = (3/4\pi)(1 - 2\chi/n^3)$. Below $\tilde{\phi}$ the scaling argument should be used. Above $\tilde{\phi}$ the solution is ideal again and the mean field method is applicable. In most experimental systems, even for flexible chains in the best solvents, $\tilde{\phi}$ is on the order of 0.01. However, the prefactor in his criterion is rather uncertain, and it may lead to larger $\tilde{\phi}$. On the other hand, in polymer adsorption the volume fraction is usually much greater than $\tilde{\phi}$ for much of the adsorbed layer. On the basis of these arguments, the mean-field theory can give accurate results in most of the cases studied in this paper. Even for semedilute solutions with good solvent, where the quantitative predictions should be modified by scaling analysis, we expect that SCFT can provide qualitatively correct results.

Strong adsorption of polymers are considered in this paper. In the numerical calculations the potential width d is taken as equal to two segments size, or, $d = 2b$, while the adsorption potential is $U_0/k_BT = -0.4$. In general, chain configurations in the proximity of surface are affected significantly by the nature of polymer−surface interaction. However, we have tested with different potentials and the results indicated that the interaction only affects the boundary layer near the surface. It has little effect on chains in adsorbed layer. In particular, the change of average tail length with curvature is nearly independent of the material nature of polymer−surface interaction as long as the interaction is strong.

Figure 1 shows the polymer density profiles near the surface at different bulk polymer concentrations. Since the parameter is taken as $\chi = 0.4$, which is close to the Θ solvent, the excluded volume interactions between segments are weak. The density profiles rise from 0 to a maximum value, and then decrease and approach to the bulk concentrations at large distance. However, our calculation do not predict a depletion hole that exists at a distance from the surface where the concentration is slightly lower than that in the bulk as the result in other reference.[18] Since the potential well is deep, the polymer density in the adsorbed layer is high even at low bulk concentration $\phi_p{}^0$. As the bulk concentration increases, the distance impacted by adsorbing potential becomes smaller and smaller. When $\phi_p{}^0$ is small, the distance is over 20 segment sizes. As $\phi_p{}^0$ approaches 1, the region impacted by adsorbing potential is only four or five segment sizes. This can be understood easily. At low bulk concentration, many segments can get together near the surface until the chemical potential reaches equilibrium. At high concentration, the interaction between segments is predominant and the solution is incompressible, which opposes the gathering together of segments. Thus, even if the interaction between segments and surface is violent, it cannot vary the density near the surface markedly.

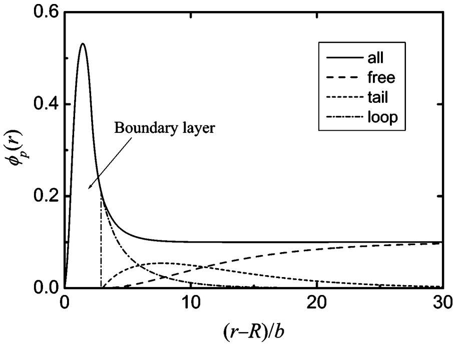

Figure 2. Polymer segments distributions belong to tail, loop, and free part. The parameters are $N = 1000$, $\phi_p{}^0 = 0.1$, $\chi = 0.4$, and $R/b = 10$.

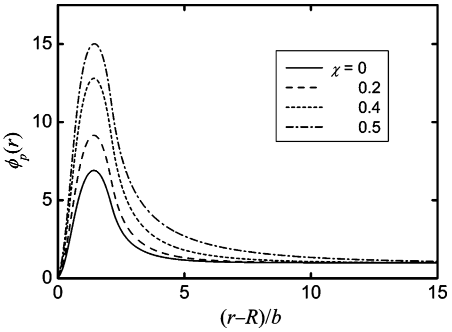

Figure 3. Effect of quality of solvents on monomer volume fraction. The parameters are $N = 1000$, $\phi_p{}^0 = 0.04$, $R/b = 10$, and $\chi = 0$, 0.2, 0.4, and 0.5, respectively.

Figure 2 shows the decomposition of the polymers density profiles into tail, loop and free parts. These results are similar to those of Fleer et al.[17] The tails are the dominant part at some distance away from the surface, while in the inner region of the absorbed layer near the surface, loops are the dominant part.

Figure 3 demonstrates how the interaction parameter χ affects the density profile near the sphere surface. We can find that when χ approaches 0.5, or the solvent property approaches to Θ solvent, the density profile is higher and broader. These profiles show the same trend as the results for graft polymers obtained by Muthukumar et al.[29]

Figures 4−6 show how the tail fraction, the average loop, and the tail length vary with the polymer chain length at two-limit particle sizes for $N \geq 50$. The bulk concentration is 0.1 and $\chi = 0$. The solid lines are for $R = 1$, in which the particle radius is much smaller than the natural size of the chains. The dash lines are for $R = 1000$, in which the particle radius is much larger than the natural size of the chains. Figure 4 indicates that the tail fraction increases with increasing N. When $N \leq 2000$ the increase is obvious and then it goes down. This means long chains have more entropy against the adsorb potential and have more parts dangling in the outer space of adsorbed layer. The particle-size effect is obvious. For smaller R, polymers have more space to move. Most of segments of adsorbed chains

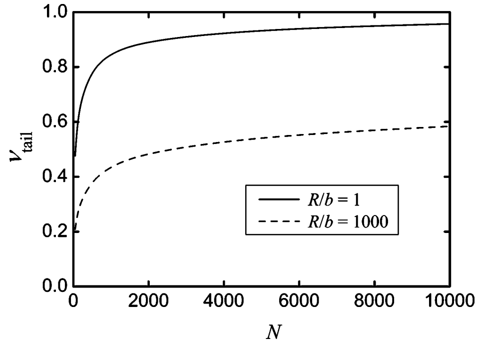

Figure 4. Fraction of tail as a function of the degree of polymerization N at two limit curvatures of $R/b = 1$ and 1000, respectively. $\chi = 0$; $\phi_p{}^0 = 0.1$.

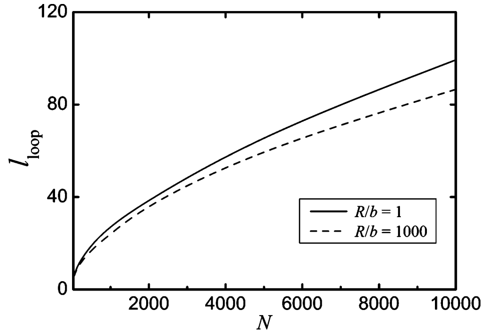

Figure 5. Average loop length as a function of the degree of polymerization N at two limit curvatures of $R/b = 1$ and 1000, respectively. $\chi = 0$; $\phi_p{}^0 = 0.1$.

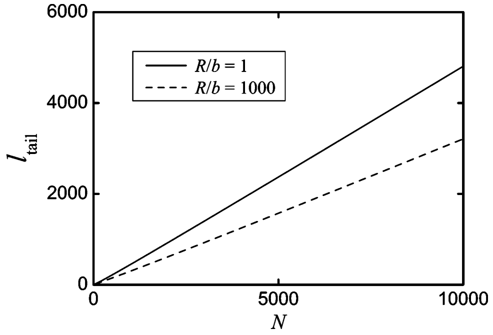

Figure 6. Average tail length as a function of the degree of polymerization N at two limit curvatures of $R/b = 1$ and 1000, respectively. $\chi = 0$; $\phi_p{}^0 = 0.1$.

belong to tails. The proportion of tails in this case is much higher than that for larger R. Figure 5 gives the average loop length as a function of N. The particle size has little effect on the average loop length. Figure 6 gives a scaling relationship between average tail length and N. Through linear fitting we find that when R is much larger than polymer coil the result is $l_{tail} \simeq 0.32N$, which is the same as the lattice model[17] and the analytic result of Johner for plate case.[30] However, when R is much smaller than polymer coil, we obtain $l_{tail} \simeq 0.48N$. This means that the particle size does not change the scaling exponent of the average tail length with N, but it affects the coefficient. The coefficient is higher for smaller curvature. Thus, when R becomes very small, most polymer segments belong to the tails.

Figure 7 presents the main results of this study. It demonstrates how the average tail length changes with the normalized particle size R/R_g at different bulk concentrations, where R_g is the chain radius of gyration and $R_g = 12.9$ for $N = 1000$. One can see that the average tail length is a decreasing function of the particle radius. This influence is distinct, especially, when the particle radius is smaller than the polymer gyration radius in solutions. This can be easily understood. When the radius increases, the dangling tails have more possibilities for contact with the surface and the tails become shorter. When the bulk concentration increases, the curvature effect will be weakened because of the excluded volume effect of polymers.

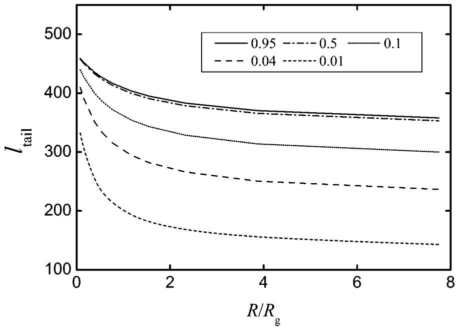

Figure 7. Average tail length as a function of normalized particle radius at different bulk concentrations of $\phi_p{}^0 = 0.01$, 0.04, 0.1, 0.5, and 0.95, respectively. $N = 1000$; $\chi = 0.2$.

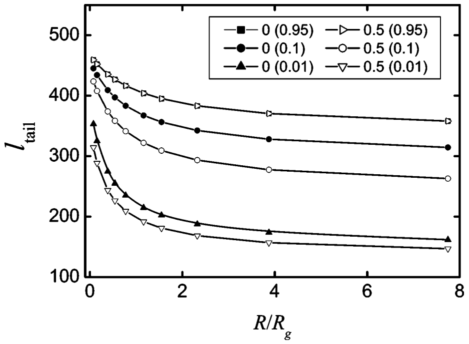

Figure 8. Average tail length as a function of normalized particle radius at three polymer bulk concentrations of $\phi_p{}^0 = 0.01$, 0.1, and 0.95, respectively. Here $N = 1000$. The lines with solid and hollow symbol are for $\chi = 0$ and 0.5, respectively. The number in the brackets represent the bulk concentrations. For $\phi_p{}^0 = 0.95$ the two lines for $\chi = 0$ and 0.5 superpose.

Figure 8 shows the effect of solvent quality on the average tail length. We calculate the average tail length with interactions parameter $\chi = 0$ and $\chi = 0.5$ at three different bulk concentrations of 0.01, 0.1, and 0.95. When bulk concentration decreases the effect of solvent becomes distinct. We can find that tails are longer in good solvent than in poor solvent. This indicates excluded volume effect enforces more segments of a chain in unconfined space. This impact is more obvious at $\phi_p{}^0 = 0.1$ than at $\phi_p{}^0 = 0.01$, because at high concentration the excluded volume effect is more insensitive. However, when the bulk concentration is high enough we can conclude that the solvent quality has little effect on the average tail length. In fact, in this case the solution is so concentrated that it has the same behavior as in melts, and the interactions between polymer segments are screened strongly so that a polymer chain can behave like a Gaussian chain.

4. Discussion

In this section, we would like to discuss a possible explanation of the effect of adding a small amount of nanoparticles to concentrated polymer solutions and polymer melts. From the calculated adsorbed layer structure, mainly the average tail and loop length at different particles radius, we can examine how these quantities affect the entanglement of polymers belonging to different particles. From above results, we find that the excess entanglements between particles should be attributed to tails

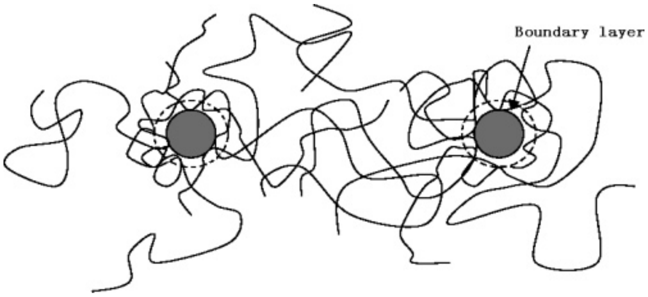

Figure 9. Schematic entanglements of tails belonging to two particles.

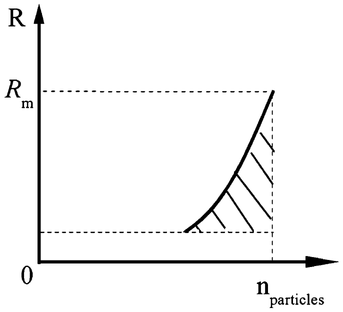

Figure 10. Schematic "phase diagram" in number density n_p and radius R of colloidal particles. The shade area is the region where the entanglements between tails occur.

instead of loops. The reason is that loops are usually short and they only affect the regions near the surface of particles. On the other hand, tails can extend to large distances and they may dominate the physical properties in the out space due to entanglements. The basic idea is that these nanoparticles can lead to excess entanglements because of the larger tail lengths. For a small amount of well-dispersed nanoparticles in concentrated polymer solutions or melts, the radius of particles is the key factor to determine the conformations of adsorbed polymers. Each dispersing nanoparticle adsorbs many polymer chains. So one particle has many tails, just like an octopus with many long tentacles. If the tails are long enough and there are no bridges among polymers, those tails (tentacles) belonging to different particles (octopuses) may entangle each other, which is shown schematically in Figure 9. This mechanism is different from that of Johner et al.[31] In their argument, a long polymer chain links several small colloid particles. The particles are attractive through bridges of polymer chains, so the whole solution becomes a gel by adsorption or separates into two phases. However, in the current case no bridge occurs and the system becomes a giant networks through excess entanglements of tails. The average tail height is denoted as H_{tail}. When the average distance between two neighbor nanoparticles l_0 is shorter than twice of H_{tail}, we can assume that the entanglements occur. If the number of particles suspension N_{part} is fixed, the average distance l_0 will relate to the density of particle number n_{part}, or, $l_0 = n_{part}^{-1/3}$. As we obtained above, increasing the radius of particles will cause the average tail length to decrease. According to the scaling relationship, we find that the average height of tails satisfies $H_{tail} = (l_{tail})^{\nu} b$. When the radius exceeds one critical value R_c, which is a function of n_{part}, the entanglements among tails belonging to two close particles will vanish. At the same time, for a given polymerization of polymer, there exists a minimum tail length at which the entanglement happens.[32] This means that there is a maximum radius R_m of the particle. When $R > R_m$, the entanglements will not occur, since the tails are not long enough, and only a few tails are larger than the colloid while the rest tails mainly entangle with the linear chains rather than the other tails. On the other hand, if the particles are too small and carry only one chain for each particle, the entanglement between the tails will be infrequent. In this case the colloid is almost irrelevant for the dynamics. Only in concentrated polymer solutions or melts, those particles with moderate size in which each of them carries many long tails, can induce the excess entanglements. Thus, we can obtain a schematic "phase diagram" as in Figure 10. In this diagram, excess entanglements occur only in the shade region. In the region, the dispersing colloidal particles behave as the entanglement points as well. The entanglements are important in determining rheological, dynamic, and fracture properties, especially for solution or melt viscosity. The excess entanglements arising from adding particles may have more important effect on solution viscosity. We can imagine that many octopuses swim in solution. Once their tentacles entangle together, one octopus hardly moves, just like the reptation of a branched polymer in concentrated solution. So the reptation time is long and the solution viscosity increases greatly. This kind of entanglement interaction must be stronger than that without adsorption. The excess entanglements will transmit more force per unit area (stress), just like the sulfureted rubber or gel. In this case we can say that the solution is cross-linked by the added particles although there is no bridge of polymers. The bridge can occur between two particles if the average distance l_0 is small enough. However, the excess entanglements will happen before the bridges form as two particles approach. In experiments, if a small amount of nanoparticles is added into polymer solutions or melts, only small particles can improve the dynamic properties of system distinctly. However, if the radius of suspensions is larger than a certain value, these particles cannot induce obvious improvement on the properties of the system. In this work, we do not calculate the number and the detailed distribution of adsorbed tails on the colloidal particles, which is essential for investigating the excess entanglement effect. Moreover, the extent of entanglement among tails has to be considered as the distance between colloids changes. Further calculations are needed for future work.

5. Conclusion

In this paper, we solved a set of self-consistent equations to study the homopolymer adsorption at spherical coordinate in solutions. The effect of particle size (surface curvature), chain length, solvent, and bulk concentrations are investigated. We found that the particle size can affect the structure of adsorbed polymer distinctly. The average loop length remains roughly as a constant at different particle radius, while the average tail length decreases with increasing particle radius. Better solvent and higher bulk concentration leads to longer tail length. If the concentration is high enough the solvent quality has little effect on the structure of adsorbed layer. For small particles with $R = 1$ the average tail length has the scaling relationship $l_{tail} \simeq 0.48N$, while for large particles with $R = 1000$, $l_{tail} \simeq 0.32N$. Adding small nanoparticles in polymer solutions or melts may improve the properties of the system by adsorption. When particles are small enough the tails belonging to different particles may entangle to each other. So the polymer solutions or melts can be a giant net through this kind of entanglements. This particle-induced entanglement occur for small particles and higher particle concentrations (Figure 10). This observation provides a possible mechanism for the reenforcement of polymer systems by nanoparticles.

Acknowledgment. We thank Prof. Z. G. Wang for stimulating discussions on this subject. YS thanks Chao Yan for the help on numerical calculation. This work is supported by the National Natural Science Foundation of China (NSFC) Nos. 20340420327, 20474074, 20490220, 20574085, and 90103037 and the 973 Project 2004CB720606. A.-C.S. acknowledges the support from Natural Science and Engineering Research Council (NSERC) of Canada.

Appendix: Numerical Solving of Modified Diffusion Equation

We solve the diffusion equation using the so-called Crank–Nicholson method. We discretize the (r, t) space into a rectangular grid in term of Δt, Δr. Thus

$$r \rightarrow r_i = i \times \Delta r + R, \quad \text{with } i = 0, 1, ..., M$$

$$t \rightarrow t_j = j \times \Delta t, \quad \text{with } j = 0, 1, ..., N$$

By this way we can obtain the discretized equations. In discretized (r, t) space of spherical coordinate the modified diffusion equation is

$$\frac{\partial}{\partial t}q(i, j) = \frac{b^2}{6}\left(\frac{\partial}{\partial r^2} + \frac{2}{r}\frac{\partial}{\partial r}\right) q(i, j) - \omega(i)q(i, j) \qquad \text{(A1)}$$

with initial condition $q(i, 0) = 1$ and boundary conditions $q(0, j) = 0$ and $q(m - 1, j) = q(m + 1, j)$. The essence of this method is to write the discretized version of the time derivative in the form

$$\frac{q(i, j + 1) - q(i, j)}{\Delta t} = \frac{1}{2}\left[\frac{\partial}{\partial t}q(i, j) + \frac{\partial}{\partial t}q(i, j + 1)\right] \qquad \text{(A2)}$$

where the time derivatives are obtained using the modified diffusion eq A1.

To make the time evolution simply we define a new intermediate quantity $u(i, j)$

$$u(i, j) = q(i, j) - \frac{\Delta t}{2}\frac{\partial}{\partial t}q(i, j) \qquad \text{(A3)}$$

Substituting eq A1 into eq A3, we can obtain

$$u(i, j) = \mathbf{A}q(i, j) + \mathbf{B}q(i + 1, j) + \mathbf{C}q(i - 1, j) \qquad \text{(A4)}$$

Here,

$$\mathbf{A} = 1 + \frac{b^2}{6}\frac{\Delta t}{(\Delta r)^2} + \frac{\Delta t}{2}\omega(i)$$

$$\mathbf{B} = -\frac{b^2}{12}\frac{\Delta t}{\Delta r}\left(\frac{1}{\Delta r} + \frac{1}{r_i}\right)$$

$$\mathbf{C} = -\frac{b^2}{12}\frac{\Delta t}{\Delta r}\left(\frac{1}{\Delta r} - \frac{1}{r_i}\right)$$

The time evolution of the system is now written in the simple form

$$u(i, j + 1) = 2q(i, j) - u(i, j) \qquad \text{(A5)}$$

Starting from the initial values of $q(i, 0) = 1$, we can compute the corresponding $u(i, 0)$ by eq A3 and $u(i, 1)$ by eq A5. Then we can solve the linear eq A3 for $q(i, j + 1)$ from the computed $u(i, j + 1)$ and boundary conditions. Since this set of linear equations has the simple trigonal form, the solution can be obtained easily from standard process.[33] Repeating the above steps we can obtain the solution for the whole $q(i, j)$.

References and Notes

(1) Napper, D. H. *Polymer Stabilization of Colloid Dispersions*; Academic Press: London, 1983.
(2) Fleer, G. J.; Cohen Stuart, M.; Schjeutjens, J. M. H. J.; Cosgrove, T.; Vincent, B. *Polymers at Interface*; Chapman and Hall: London, 1993.
(3) Johner, A.; Joanny, J. F.; Orrite, S. D.; Avalos, J. B. *Europhys. Lett.* **2001**, *56*, 549.
(4) Wijmans, C. M.; Zhulina, E. B. *Macromolecules* **1993**, *26*, 7214.
(5) Aubouy, A.; Raphael, E. *Macromolecules* **1998**, *31*, 4357.
(6) Ji, H.; Hone, D. *Macromolecules* **1988**, *21*, 2600.
(7) Skau, K. I.; Blokhuis, E. M. *Macromolecules* **2003**, *36*, 4637.
(8) de Gennes, P. G. *Scaling Concepts in Polymer Physics*; Cornel1 University Press: Ithaca, NY, 1979.
(9) de Gennes, P. G. *Rep. Prog. Phys.* **1969**, *32*, 187.
(10) Jones, I. S.; Richmod, P. J. *J. Chem. Soc., Faraday Trans. 2*, **1977**, *73*, 1062.
(11) de Gennes, P. G. *Macromolecules* **1981**, *14*, 1637. de Gennes, P. G. *Macromolecules* **1982**, *15*, 492.
(12) de Gennes, P. G. *Adv. Colloid Interface Sci.* **1987**, *27*, 719.
(13) Eisenriegler, E. *Polymers near interfaces*; World Scientific: Singapore, 1993.
(14) Eisenriegler, E.; Kremer, K.; Binder, K. *J. Chem. Phys.* **1986**, *77*, 6296.
(15) Eisenriegler, E. *J. Chem. Phys.* **1983**, *79*, 1052; **1984**, *81*, 4666; **1985**, *82* 1032.
(16) Scheutjens, J.; Fleer, G. J. *J. Phys. Chem.* **1979**, *83*, 1619.
(17) Scheutjens, J.; Fleer, G. J. *J. Phys. Chem.* **1980**, *84*, 178.
(18) Semenov, A. N.; Joanny, J. F.; Johner, A.; Grosberg, A. *Theoretical and Mathematical Models in Polymer Research*; Academic Press: San Diego, CA, 1998.
(19) Clement, F.; Johner, A. *C. R. Acad. Sci. Paris*, *t.1, Ser. 4* **2000**, 1135.
(20) Daoullas, K. C.; Theodorou, D. N.; Harmandaris, V. A.; Karayiannis, N. C.; Mavrantzas, V. G. *Macromolecules* **2005**, *38*, 7134.
(21) Mavrantzas, V. G.; Beris, A. N.; Leermakers, F.; Fleer, G. J. *J. Chem. Phys.* **2005**, *123*, 174901.
(22) Semenov, A. N.; Bonet-Avalos, J.; Johner, A.; Joanny, J. F. *Macromolecules* **1996**, *29*, 2179. Joanny, J. F.; Johner, A.; Bonet-Avalos, J. *Macromolecules* **1997**, *30*, 1479.
(23) Stuart, M. A. C.; Waajen, F. W. H.; Cosgrove, T.; Vincent, B.; Crowley, T. L. *Macromolecules* **1984**, *17*, 1825.
(24) Hong, K. M.; Noolandi, J. *Macromolecules* **1981**, *14*, 727.
(25) Whitmore, M. D.; Noolandi, J. *Macromolecules* **1990**, *23*, 3321.
(26) Doi, E.; Edwards, S. F. *The Theory of Polymer Dynamics*, Clarendon Press: Oxford, U.K., 1986.
(27) Schaefer, D. W. *Polymer* **1984**, *25*, 387.
(28) Scheutjens, J.; Fleer, G. J.; Cohen Stuart, M. A. *Colloids Surf.* **1986**, *21*, 285.
(29) Muthukumar, M.; Ho, Jyh-Shyong. *Macromolecules* **1989**, *22*, 965.
(30) Johner, A.; Joanny, J.-F.; Rubinstein, M. *Europhys. Lett.* **1993**, *22*, 591.
(31) Johner, A.; Joanny, J. F.; Diez, S.; Bonnet-Avalos, J. *Europhys. Lett.* **2001**, *56*, 549.
(32) Kavassalis, T. A.; Noolandi, J. *Macromolecules* **1989**, *22*, 2709.
(33) Press, W. H.; Teukolsky, S. A.; Vetterling, W. T.; Flannery, B. P. *Numerical Recipes in C*, 2nd ed.; Cambridge University Press: Cambridge, U.K., 1997.

MA060014A